Engineering Microbiology 3 (2023) 100086

Contents lists available at ScienceDirect

Engineering Microbiology

journal homepage: www.elsevier.com/locate/engmic

Original Research Article

Yeast surface display of leech hyaluronidase for the industrial production of hyaluronic acid oligosaccharides

Lizhi Liao[a,b], Hao Huang[a], Yang Wang[a,b,*], Guocheng Du[b,c], Zhen Kang[a,b,*]

[a] The Science Center for Future Foods, Jiangnan University, Wuxi 214122, China
[b] The Key Laboratory of Carbohydrate Chemistry and Biotechnology, Ministry of Education, School of Biotechnology, Jiangnan University, Wuxi 214122, China
[c] The Key Laboratory of Industrial Biotechnology, Ministry of Education, School of Biotechnology, Jiangnan University, Wuxi 214122, China

ARTICLE INFO

Keywords:
Hyaluronan
Leech hyaluronidase
Yeast display
Biocatalysis
Enzyme immobilization

ABSTRACT

Leech hyaluronidase (LHyal) is a hyperactive hyaluronic acid (HA) hydrolase that belongs to the hyaluronoglucuronidase family. Traditionally, LHyal is extracted from the heads of leeches, but the recent development of the *Pichia pastoris* recombinant LHyal expression method permitted the industrial production of size-specific HA oligosaccharides. However, at present LHyal expressed by recombinant yeast strains requires laborious protein purification steps. Moreover, the enzyme is deactivated and removed after single use. To solve this problem, we developed a recyclable LHyal biocatalyst using a yeast surface display (YSD) system. After screening and characterization, we found that the cell wall protein Sed1p displayed stronger anchoring to the *P. pastoris* cell wall than other cell wall proteins. By optimizing the type and length of the linkers between LHyal and Sed1p, we increased the activity of enzymes displayed on the *P. pastoris* cell wall by 50.34% in flask cultures. LHyal-$(GGGS)_6$-Sed1p activity further increased to 3.58×10^5 U mL^{-1} in fed-batch cultivation in a 5 L bioreactor. Enzymatic property analysis results revealed that the displayed LHyal-$(GGGS)_6$-Sed1p generated the same oligosaccharides but exhibited higher thermal stability than free LHyal enzyme. Moreover, displayed LHyal-$(GGGS)_6$-Sed1p could be recovered easily from HA hydrolysis solutions via low-speed centrifugation and could be reused at least 5 times. YSD of LHyal not only increased the utilization efficiency of the enzyme but also simplified the purification process for HA oligosaccharides. Thus, this study provides an alternative approach for the industrial preparation of LHyal and HA oligosaccharides.

1. Introduction

Hyaluronic acid (HA) is a high molecular weight, negatively charged polysaccharide composed of glucuronic acid and N-acetyl-glucosamine. High molecular weight HA (HMW-HA) is universally found in the extracellular matrices of mammalian tissue and displays strong water binding and lubricating biophysical activities. In nature HA is degraded by hyaluronidases and generates HA fragments of different molecular weights [1]. Compared to HMW-HA, low molecular weight HA (LMW-HA, 10^4–10^5 Da) shows lower water binding and lubricating activity but stronger biological activity; it is frequently used in cosmetic products to increase the skin elasticity and reduce wrinkles [2,3]. HA oligosaccharides (molecular weight ≤ 10^4 Da) are readily absorbed by the human body [4,5]. Recently, the preparation of LMW-HA via hyaluronidase digestion has attracted considerable research attention.

Hyaluronidases can be roughly classified into three main groups, HA lyases, hyaluronoglucosaminidase, and hyaluronoglucuronidases, based on their catalytic mechanism [5]. Many of these enzymes have been used to degrade HMW-HA into LMW-HA [6]. For example, Leech hyaluronidase (LHyal), which is extracted from the heads of leeches, has been characterized as a hyaluronoglucuronidase. It specifically cleaves the β−1,3-glycosidic bonds that connect D-glucuronate and N-acetyl-D-glucosamine residues in HA [7,8]. After elucidating the coding sequence of LHyal, recent work has focused on expressing LHyal in microbes, to be used for the enzymatic production of LMW-HA from HMW-HA [8–14]. LHyal displays desirable traits, including high enzyme activity, high substrate specificity, and a lack of trans-glycosidase activity [8]. LHyal produces the specific molecular weight HA and does not display any risks of animal cross-infection [8,14]. Therefore, large-scale industrial production of recombinant LHyal offers great promise for industrial-scale productions of HA oligosaccharides [8,10,14].

However, industrial application of LHyal to produce LMW-HA is restricted by the high cost of purifying proteins at scale. Moreover, although LHyal retains considerable residual activity after HA digestion, the enzyme is deactivated and removed after a single use. Enzyme immobilization is a general strategy used to improve enzyme recycling

* Corresponding authors.
E-mail addresses: y.wang@jiangnan.edu.cn (Y. Wang), zkang@jiangnan.edu.cn (Z. Kang).

https://doi.org/10.1016/j.engmic.2023.100086
Received 15 March 2023; Received in revised form 3 April 2023; Accepted 4 April 2023
Available online 5 April 2023

Table 1
Plasmids used in this study.

Plasmids	Property description	Source
pGAP(m)-*sp23-LHyal*	*HIS4 Amp*^{r} *and Kan.*^{r}	[11]
pPIC9K-*GFP*	*HIS4 Amp*^{r} and *Kan*^{r}	This work
pGAP(m)-*sp23-LHyal-Gcw51p*	Based on pGAP(m)-*sp23-LHyal*, with *Gcw51p* fused to the C-terminal of *LHyal*	This work
pGAP(m)-*sp23-LHyal-Sed1p*	Based on pGAP(m)-*sp23-LHyal*, with *Sed1p* fused to the C-terminal of *LHyal*	This work
pGAP(m)-*sp23-Pir1p-LHyal*	Based on pGAP(m)-*sp23-LHyal*, with *Pir1p* fused to the N-terminal of *LHyal*	This work
pGAP(m)-*sp23-GFP-Gcw51p*	Based on pGAP(m)-*sp23-LHyal-Gcw51p* with *LHyal* replaced with *GFP*	This work
pGAP(m)-*sp23-GFP-Sed1p*	Based on pGAP(m)-*sp23-LHyal-Sed1p* with *LHyal* replaced with *GFP*	This work
pGAP(m)-*sp23-Pir1p-GFP*	Based on pGAP(m)-*sp23-Pir1p-LHyal* with *LHyal* replaced with *GFP*	This work
pGAP(m)-*sp23-LHyal*-$(GGGS)_3$-*Sed1p*	Based on pGAP(m)-*sp23-LHyal-Sed1p* with $(GGGS)_3$ linker inserted between *LHyal and Sed1p*	This work
pGAP(m)-*sp23-LHyal*-S2-*Sed1p*	Based on pGAP(m)-*sp23-LHyal-Sed1p* with S2 linker inserted between *LHyal and Sed1p*	This work
pGAP(m)-*sp23-LHyal*-L1-*Sed1p*	Based on pGAP(m)-*sp23-LHyal-Sed1p* with L1 linker inserted between *LHyal and Sed1p*	This work
pGAP(m)-*sp23-LHyal*-R1-*Sed1p*	Based on pGAP(m)-*sp23-LHyal-Sed1p* with R1 linker inserted between *LHyal and Sed1p*	This work
pGAP(m)-*sp23-LHyal*-$(EAAAK)_3$-*Sed1p*	Based on pGAP(m)-*sp23-LHyal-Sed1p* with $(EAAAK)_3$ linker inserted between *LHyal and Sed1p*	This work
pGAP(m)-*sp23-LHyal*-PT-*Sed1p*	Based on pGAP(m)-*sp23-LHyal-Sed1p* with PT linker inserted between *LHyal and Sed1p*	This work
pGAP(m)-*sp23-LHyal*-$(GGGS)_6$-*Sed1p*	Based on pGAP(m)-*sp23-LHyal-Sed1p* with $(GGGS)_6$ linker inserted between *LHyal and Sed1p*	This work
pGAP(m)-*sp23-LHyal*-$(GGGS)_9$-*Sed1p*	Based on pGAP(m)-*sp23-LHyal-Sed1p* with $(GGGS)_9$ linker inserted between *LHyal and Sed1p*	This work
pGAP(m)-*sp23-LHyal*-$(GGGS)_{12}$-*Sed1p*	Based on pGAP(m)-*sp23-LHyal-Sed1p* with $(GGGS)_{12}$ linker inserted between *LHyal and Sed1p*	This work

efficiency. Adsorption is a simple method that fixes proteins to a solid surface via non-covalent interactions [15]. Although the structure of the enzyme is unlikely to be affected, interactions between the carrier material and the enzyme are rather weak and may block contact between the enzyme and reaction substrate [16]. In general, enzymes used for fixation must be purified before adsorption, but some surface display techniques have been developed for enzyme immobilization that do not require protein purification. Yeast strains are excellent hosts for enzyme display because they are also used as hosts for protein overproduction and can be easily collected [17].

In this study, we developed a recyclable LHyal biocatalyst protocol using a *P. pastoris* yeast surface display (YSD) system to facilitate the isolation and reuse of LHyal. After protein expression and secretion, LHyal was immediately immobilized to the cell surface of *P. pastoris* via cell wall anchor proteins. This YSD system showed high enzyme activity and reusability. To demonstrate this, we used highly active LHyal as an efficient biocatalyst for preparing HA oligosaccharides. After optimization, this system produced as much as 3.58×10^5 U mL^{-1} LHyal-$(GGGS)_6$-Sed1p via fed-batch fermentation.

2. Materials and methods

2.1. Chemicals and reagents

PrimeSTAR HS (Premix) and a ClonExpress^{TM} II One Step Cloning Kit were obtained from TaKaRa Bio (Dalian, China) and Vazyme Biotech (Nanjing, China), respectively. Geneticin (G418) and HMW-HA were obtained from Sangon Biotech (Shanghai, China). Primer synthesis, gene synthesis, and DNA sequencing were performed using GENEWIZ (Suzhou, China). All other chemicals used in this study were purchased from Sinopharm Chemical Reagent Co., Ltd (Shanghai, China).

2.2. Plasmid and strain construction

All plasmids and primers used in this study are listed in Tables 1 and 2. Plasmid pGAP(m)-*sp23-LHyal*, which was used for the expression of free LHyal [11], *P. pastoris* GS115, and the *Saccharomyces cerevisiae* S288C strain used for this study were all stored in our laboratory. *Gcw51p*, a gene encoding a 193aa protein fragment with its signal peptide removed [18] was obtained by PCR using the Gcw51p-F/R primers to PCR-specific DNA sequences from the *P. pastoris* GS115 genome. *Sed1p*, a gene encoding a 229aa fragment with its signal peptide removed [19] and *Pir1p*, which encodes a 323aa fragment with its signal peptide removed [20] were amplified from the genome of *S. cerevisiae* S288C by PCR using the primers Sed1p-F/R and Pir1p-F/R, respectively. According to previous study, the N-terminus of Pir1p contains SQIGDGQIQAT repeats, which are essential for the anchoring of Pir1p to the cell wall, therefore we fused the proteins GFP and LHyal to the C-terminus of Pir1p. The C-terminus of GPI type anchor protein contains a GPI signal sequence responsible for anchoring to the cell wall through the glucan connection, Gcw51p and Sed1p are connected to the C-terminus of LHyal. PCR-amplified fragments of the *Gcw51p, Sed1p*, and *Pir1p* genes were then ligated to the plasmid backbone of a pGAP(m)-*sp23-LHyal* vector using a one step cloning kit to obtain the corresponding plasmids pGAP(m)-*sp23-LHyal-Gcw51p*, pGAP(m)-*sp23-LHyal-Sed1p*, and pGAP(m)-*sp23-Pir1p-LHyal*, respectively.

Green fluorescent protein (GFP) was synthesized as pPIC9K-*GFP* by Suzhou GENEWIZ. A *GFP* fragment was obtained via PCR using GFP-F/R primer amplification with the plasmid PIC9K-*GFP* used as a template. We replaced the *LHyal* coding region of pGAP(m)-*sp23-LHyal-Gcw51p*, pGAP(m)-*sp23-LHyal-Sed1p*, and pGAP(m)-*sp23-Pir1p-LHyal* with the *GFP* sequence to obtain the corresponding plasmids pGAP(m)-*sp23-GFP-Gcw51p*, pGAP(m)-*sp23-GFP-Sed1p*, and pGAP(m)-*Pir1p-GFP*, respectively.

The coding sequences of the $(GGGS)_3$ linker, S2 linker [21], L1 linker [22], R1 linker [23], $(EAAAK)_3$ linker [18], and PT linker [24] were ligated onto the pGAP(m)-*sp23-LHyal-Sed1p* backbone via PCR using primers $(GGGS)_3$-F/R, S2-F/R, L1-F/R, R1-F/R, $(EAAAK)_3$-F/R, and PT-F/R, respectively. This ligation yielded the corresponding plasmids, pGAP(m)-*sp23-LHyal*-$(GGGS)_3$-*Sed1p*, pGAP(m)-*sp23-LHyal*-S2-*Sed1p*, pGAP(m)-*sp23-LHyal*-L1-*Sed1p*, pGAP(m)-*sp23-LHyal*-R1-*Sed1p*, pGAP(m)-*sp23-LHyal*-$(EAAAK)_3$-*Sed1p*, and pGAP(m)-*sp23-LHyal*-PT-*Sed1p*, respectively. Plasmids expressing GGGS linkers of different lengths were constructed using primers (GGGS)n (i.e., where $n = 6$, 9, or 12)-F/R to obtain plasmids pGAP(m)-*sp23-LHyal*-$(GGGS)_6$-*Sed1p*, pGAP(m)-*sp23-LHyal*-$(GGGS)_9$-*Sed1p*, and pGAP(m)-*sp23-LHyal*-$(GGGS)_{12}$-*Sed1p,* respectively.

Plasmids were then transferred into competent *P. pastoris* GS115 via electroporation after being linearized by digestion with SalI. After screening on minimal dextrose (MD) and yeast extract peptone dextrose (YPD) plates with 4 mg/mL geneticin (G418), we selected the correct recombinant strains for further analyses.

2.3. Growth media

Escherichia coli strains for cloning recombinant plasmids were cultivated in LB medium (5 g L^{-1} yeast extract, 10 g L^{-1} tryptone, and 10 g L^{-1} NaCl) at 37°C. YPD medium (10 g L^{-1} yeast extract, 20 g L^{-1} tryptone, and 20 g L^{-1} glucose) was used for yeast cultivation. MD medium (13.4 g L^{-1} yeast nitrogen base (YNB), 20 g L^{-1} dextrose, 4×10^{-4} g L^{-1} biotin, and 20 g L^{-1} agar) was used for screening *P. pastoris* GS115 recombinant strains. Modified buffered glycerol-complex (BMGY) medium (10 g L^{-1} yeast extract, 20 g L^{-1} tryptone, 13.4 g L^{-1} YNB, 4×10^{-4} g

Table 2
Primers used in this study for PCR.

Primer	Sequences (5′–3′)
Gcw51p-F	GAAGCGTGCAAAAAGATGACGATGACTCATTACCTTTTGTTATTGTTAAC
Gcw51p-R	CTAGGGAATTCTTAGATCAATAGGGCAATGGCAACACCAC
Sed1p-F	GAAGCGTGCAAAAAGCAATTTTCCAACAGTACATCTGCTTCTTCC
Sed1p-R	CCTAGGGAATTCTTATAAGAATAACATAGCAACACCAGCCAAACC
Pir1p-F	GTTGGCCTTTGCTATCTTTACTACTTTATGCATAGTTGTCCTATCTTCTC
Pir1p-R	GTGGTGGTGGTGGTGGTGACAGTTGAGCAAATCGATAGCTTGTAGG
GFP-F	CGTTGGCCTTTGCTATGGGTAAGGGAGAAGAACTTTTCACTG
GFP-R	CTAGGGAATTCTTATTTGTATAGTTCATCCATGCCATGTGTAATCC
GFP-Gcw51p-F	GATTTGCTGAATTGCATGTCTAAAGGTGAGGAGCTTTTTACGG
GFP-Gcw51p-R	GAGTCATCGTCGTCTTTGTATAACTCGTCCATGCCATGTGTTATTCC
GFP-Sed1p-F	CGTTGGCCTTTGCTATGAGCAAAGGAGAAGAACTTTTCACTGG
GFP-Sed1p-R	GTACTGTTGGAAAATTGTTTGTAGAGCTCATCCATGCCATGTG
Pir1p-GFP-F	GATTTGCTGAATTGCATGTCTAAAGGTGAGGAGCTTTTTACGG
Pir1p-GFP-R	TCGCGGCCGCTTATTTGTATAACTCGTCCATGCCATGTG
$(GGGS)_3$-F	ATCTACTGAACTGTGGCGGAGGCTCAGGCGGAGGAGGTTCAGGCGGTGGAGGTAGTGG
$(GGGS)_3$-R	CGATCTCTTTCATACTGCCTCCTCCTCCTGATCCTCCACCACTGCCTCCACCG
S2-F	GAAGCGTGCAAAAAGGAGGGTAAGTCATCTGGTTCTGAATCTAAATCTACC
S2-R	TACTGTTGGAAAATTGGGTAGATTTAGATTCAGAACCAGATGACTTACCCTC
L1-F	GATGCAAATGTTGAAGCGTGCAAAAAGTCCGGCTCTGTTACCTCTACTTCAAAGAC
L1-R	CCACGGCCAAGACTTCTACCTCAACCCAATTTTCCAACAGTACATCTGCTTCTTCCAC
R1-F	GCAAATGTTGAAGCGTGCAAAAAGATGCAGTTTAAATCCATCGTCTTGACTTTAG
R1-R	TGGAAGAAGCAGATGTACTGTTGGAAAATTGAGCTTGAGCTACTGTTACAGCAGC
$(EAAAK)_3$-F	TGAAGCGTGCAAAAAGGAAGCTGCTGCCAAGGAAGCTGCCGCCAAGGAAGCAG
$(EAAAK)_3$-R	GTCGGATTCTGGAGCTTCGGTTGGAGTAGGAGTGGTTGGAGGTGTTGTAGGAGGAGTAGG
PT-F	GAAGCGTGCAAAAAGCCTACTCCTCCTACAACACCTCCAACCACTCCTACTCCAACC
PT-R	CCTACTCCTCCTACAACACCTCCAACCACTCCTACTCCAACCGAAGCTCCAGAATCCGAC
$(GGGS)_6$-F	GCGTGCAAAAAGGGAGGTGGAGGATCCGGTGGTGGAGGATCCGGTGGTGGAGGCTCCGGTGGTGGTGGTTC
$(GGGS)_6$-R	GGATTCTGGAGCTTCTGAACCACCTCCACCAGAACCACCACCGCCAGATCCACCACCACCT
$(GGGS)_9$-F	GAAGCGTGCAAAAAGGGTGGTGGATCAGGAGGTGGATCCGGAGGTGGATCTGGTGGTGGCTCAGGTGGAGGATCA
$(GGGS)_9$-R	GTCGGATTCTGGAGCTTCTGATCCTCCACCACTACCTCCTCCAGAACCACCACCGGAACCTCCACC
$(GGGS)_{12}$-F	GTGGTGGAGGATCAGGTGGAGGTTCAGGTGGTGGATCTGGAGGTG
$(GGGS)_{12}$-R	GGATTCTGGAGCTTCACTGCCACCTCCAGATCCACCACCTGAACCTC

L^{-1} biotin, 40 g L^{-1} glycerol, and 100 mM potassium phosphate, pH 6.0) was used for shake flask cultivation of recombinant yeast strains. The *P. pastoris* GS115 recombinant strain was subjected to fed-batch fermentation using basal salt medium (BSM) containing 40 g L^{-1} glycerol, 27 mL L^{-1} H_3PO_4, 18 g L^{-1} K_2SO_4, 14.9 g L^{-1} $MgSO_4{\cdot}7H_2O$, 4.13 g L^{-1} KOH 0.93 g L^{-1} $CaSO_4$, and 4.4 mL L^{-1} particular trace metal solution (PTM1). PTM1 contained 6 g L^{-1} $CuSO4{\cdot}5H_2O$, 0.09 g L^{-1} KI, 0.02 g L^{-1} H_3BO_3, 0.2 g L^{-1} $MoNa_2O_4{\cdot}2H_2O$, 3 g L^{-1} $MnSO_4{\cdot}H_2O$, 65 g L^{-1} $FeSO_4{\cdot}7H_2O$, 0.5 g L^{-1} $CoCl_2$, 20 g L^{-1} $ZnCl_2$, 0.2 L^{-1} biotin, and 5.0 mL L^{-1} H_2SO_4.

2.4. Shake flask fermentation and fed-batch fermentation

To prepare seed cultures, single colonies of recombinant yeast strains were inoculated into 25 mL of YPD liquid medium loaded into 250 mL shake flasks and cultured for 24 h at 220 rpm and 30°C in an oscillating incubator. The seeds were then transferred to 40 mL BMGY medium at 10% (v/v) and cultured at 220 rpm and 30°C for 84 h.

For fed-batch fermentation, seed cultures were first prepared in 50 mL liquid YPD medium by shaking at 220 rpm and 30°C for 24 h, then transferred to a 5 L bioreactor (Shanghai Baoxing Bio-Engineering Equipment Co., Ltd, Shanghai, China) containing 1.8 L BSM medium. During fed-batch fermentation, ammonium hydroxide (25%) was fed automatically to maintain the pH at 5.0. Dissolved oxygen (DO) was maintained above 30% by manual adjustment of the agitation and air flow. When the DO rebounded, which indicated glycerol exhaustion, 75% (w/v) glycerol supplemented with 1.2% PTM1 was fed at a constant rate of 8 mL/L/h. Sampling was performed every 6 h to analyze dry cell weight (DCW) and enzyme activity.

2.5. Microscopy and flow cytometry analyses

For optical microscopy, yeast cells were loaded on a slide containing agarose and viewed using an Eclipse Ni-E microscope (Nikon, Tokyo, Japan) equipped with a phase-contrast microscopy module. Micrographs obtained were processed using ImageJ version 1.53t [25].

For flow cytometry analysis, yeast cells were washed three times and resuspended in phosphate buffer saline (PBS; $Na_2HPO_4{\cdot}12H_2O$, KH_2PO_4, NaCl, KCl, pH 7.4) after termination of fermentation. Samples were then diluted to an optical density at 600 nm (OD_{600}) of 0.3 and analyzed by Flow Cytometry on a cell sorter (BD Influx, USA) with *P. pastoris* GS115 used as a negative control. Flow Cytometry analysis results were processed using FlowJo version 10.8.1.

2.6. Enzyme activity assays

Recombinant yeast cells displaying LHyal were centrifuged at 5000 rpm for 2 min, washed three times, then resuspended and diluted in PBS (pH 7.4). The supernatants were pooled to analyze LHyal released into the culture broth. Enzyme activity was tested in aliquots of 1 mL reaction buffer containing 800 μL of 2 mg mL^{-1} HA dissolved in 50 mM citrate buffer (pH 5.5) with either 200 μL of the yeast cell resuspension (diluted appropriately according to OD_{600}) or 200 μL supernatant. Heat-killed yeast cells or supernatant were used as controls. The enzyme activity of LHyal was then determined using the 3, 5-dinitrosalicylic acid method to quantify the amount of reducing sugar released by HA using glucose as a standard. Activity units (U) for LHyal was defined such that one unit of enzyme activity was required to hydrolyze HA to produce 1.0 μg of reducing sugar (i.e., in glucose equivalents) per hour at 38°C [8].

2.7. HA molecular weight assay using high-performance size-exclusion chromatography

Recombinant cells displaying LHyal-$(GGGS)_6$-Sed1p were applied by 8×10^3 U mL^{-1}, 1.6×10^4 U mL^{-1}, 3.2×10^4 U mL^{-1}, 1.6×10^5 U mL^{-1}, and 3.2×10^5 U mL^{-1} to hydrolyze 10 g L^{-1} HA (~2000 kDa), at 38°C, pH 5.5 for 5 h. Samples were taken at 0.5 h, 1 h, 2 h, 3 h, 4 h, and 5 h; all

samples were centrifuged shortly after being taken. The supernatants of all samples were then filtered using a 0.22 μm-pore filter and the molecular weight of HA after hydrolysis was analyzed using high-performance size-exclusion chromatography (HPSEC). To do so, the supernatant was injected onto an Ultrahydrogel^{TM} column (300 mm × 7.8 mm i.d., Waters Corporation, Milford, MA, USA) and HPSEC was performed using a mobile phase of 0.1 M $NaNO_3$ and a flow rate of 0.9 mL min^{-1}, 25°C [25,26].

2.8. Electrospray ionization-mass spectrometry (ESI-MS) analysis of the reaction products of HA hydrolyzed by LHyal-$(GGGS)_6$-Sed1p

Next, to analyze the reaction products generated by LHyal-$(GGGS)_6$-Sed1p, 10 g L^{-1} HA (~2000 kDa) was digested with 1.0×10^4 U mL^{-1} LHyal-$(GGGS)_6$-Sed1p for 12 h. Samples were processed as described above (i.e., for HPSEC) but were instead analyzed using Waters MALDI Synapt Q-TOF mass spectrometry with an analytical reverse-phase CSH C18 column (130 Å, 2.1 × 50 mm, 1.7 μm; Waters). The mobile phase A consisted of 0.1 M ammonium formate and the mobile phase B consisted of acetonitrile. The chromatographic run featured mobile phase B concentrations ranging from 0% to 90% for linear elution over the course of 10 min at a flow rate of 0.3 mL min^{-1}. MassLynx software (version 4.1) was used to analyze data from all processed samples data [12].

3. Results

3.1. Selection of anchor proteins for LHyal yeast surface display

Yeast surface display is a powerful biotechnology used to isolate and stabilize proteins [27–29]. Most target and anchor proteins are displayed on the surface of yeast cells as fusion proteins. Anchor proteins use serine- and threonine-rich regions and C-terminus GPI domains to display the target protein on the cell surface [30]. These anchor proteins used has important effects on-cell adhesion, morphological changes, and cell wall synthesis [31,32]. Anchor proteins were first discovered in *S. cerevisiae* [30], and later in *Yarrowia lipolytica* [33] and *P. pastoris* [18].

To construct a YSD system suitable for LHyal, we selected three yeast cell wall proteins that had been identified in previous studies [18–20]. The selected proteins included Gcw51p, which is encoded in the *P. pastoris* GS115 genome, and two anchor proteins, Sed1p and Pir1p, which are encoded in the *S. cerevisiae* S288C genome. LHyal was fused to the C- and N-terminus of these selected anchor proteins, respectively (Fig. 1a and 1b).

We first used GFP to evaluate whether glycosylphosphatidylinositol (GPI)-anchored domains could display heterogenous proteins. Under the microscope, we found that cells carrying the plasmids pGAP(m)-*sp23-GFP-Gcw51p*, pGAP(m)-*sp23-GFP-Sed1p*, and pGAP(m)-*sp23-Pir1p-GFP* exhibited different GFP fluorescence signals (Fig. 1c). Flow cytometry analysis showed that the fluorescent signals emitted from the three strains showed different offsets compared to the negative control strain (*P. pastoris* GS115); we identified GFP-Sed1p as the best construct (Fig. 1d).

Using a similar process, we displayed LHyal on the surface of *P. pastoris*. We then assayed the relative activity of LHyal released into the medium and attached to the cell surface. We found that LHyal was successfully anchored on the yeast surface by all three GPI domains (Fig. 1e). Moreover, yeast cells expressing LHyal-Sed1p displayed the highest activity, which was 3.48% and 72% higher than the activities of LHyal-Gcw51p and Pir1p-LHyal, respectively. Therefore, LHyal-Sed1p was used for subsequent experiments.

3.2. Optimization of linkers to enhance YSD LHyal expression

Linker peptides on the surface display system can generally improve enzyme activity by increasing the chance of contact with the substrate or by decreasing the interference of the anchor protein on the target protein [24,34]. The flexibility and length of linkers is often manipulated during surface display optimization because it has an important effect on the bioactivity of multifunctional proteins. Considering that the cell wall fusion protein may influence the activity of LHyal, we assessed whether the activity of LHyal displayed on the cell surface could be enhanced via the addition of linkers between the anchor protein and LHyal. To this end, we designed six linkers, including the $(GGGS)_3$ linker, S2 linker (EGKSSGSESKST), the L1 linker (SGSVTSTSKTTAKTSTST), the $(EAAAK)_3$ linker, the PT linker (PTPPTTPPTTPTPT), and the R1 linker (MQFKSIVLTLAAVTVAQA). Each of these linkers was inserted between LHyal and Sed1p to construct different LHyal-(linker)-Sed1p protein hybrids (Fig. 2b). Structural models for each of these protein hybrids were created using DeepMind AlphaFold [35] These protein models suggested that all protein constructs should fold into compact and stable three-dimensional structures (Fig. 2a). The spatial coordination of LHyal and Sed1p were quite different when different linkers were used, but the structure of LHyal seemed to be unaffected by the addition of linkers (Fig. 2b).

The enzyme activity of LHyal-(linker)-Sed1p was found to be strongly influenced by different linker types. The incorporation of a $(GGGS)_3$ linker increased the enzyme activity of the YSD system by 30.4% compared to LHyal-Sed1p, which contained no protein linker. The GGGS linker includes both glycine (Gly) and serine (Ser) residues, which provide flexibility [36], which may relieve interference of the anchor protein on the target protein.

The activity of LHyal-(linker)-Sed1p was influenced not only increased by linker type, but also by linker length [37,38]. Four linker peptides of different amino acid unit lengths were constructed using the flexible linker unit GGGS. LHyal-$(GGGS)_6$-Sed1p performed the best, increasing the activity of LHyal-Sed1p by 50.34% relative to the no-linker control (Fig. 2c). These results indicated that a GGGS linker with 24 amino acids was the most suitable for the LHyal-Sed1p YSD system.

3.3. Depolymerization of HWM-HA produced by yeast surface-displayed LHyal

Next, we analyzed the hydrolysis process of HMW-HA (~2000 kDa, at 10 g L^{-1}) by different amounts of yeast surface-displayed LHyal. We found the molecular weight of HA decreased rapidly during the first hour of interaction with different amounts of LHyal-$(GGGS)_6$-Sed1p. Afterward, molecule weight stabilized at just under 10 kDa (Fig. 3a). Therefore, it was necessary to control both the amount of LHyal-$(GGGS)_6$-Sed1p and the hydrolysis time in order to prepare HAs of different molecular weights.

According to previous studies, the final products of LHyal hydrolysis of HA are tetrasaccharides ($HA4^{NA}$), hexasaccharides ($HA6^{NA}$), and a small number of disaccharides ($HA2^{NA}$) [8,12]. The total ion flow chromatogram of the final products of HA hydrolysis with LHyal-$(GGGS)_6$-Sed1p generated three separate peaks (Fig. 3b). Analysis of the mass spectra of each peak showed that these three peaks represented HA^{NA}-type di- (Fig. 3c), tetra- (Fig. 3d), and hexasaccharides (Fig. 3e), respectively. Mass spectrometry results confirmed that LHyal-$(GGGS)_6$-Sed1p was able to hydrolyze HA to produce disaccharides, which is the same final product as is produced by HA hydrolysis using free LHyal [12].

3.4. Enzymatic characterization of yeast surface-displayed LHyal

To further evaluate the performance of YSD LHyal, we investigated the influences of two major factors on enzyme catalytic activity: temperature and pH. Surface-displayed LHyal-$(GGGS)_6$-Sed1p and free LHyal showed the same optimum reaction temperature (45°C), while LHyal-$(GGGS)_6$-Sed1p showed considerably higher activity at temperatures higher than 50°C (Fig. 4a). Moreover, surface-displayed LHyal-$(GGGS)_6$-Sed1p and free LHyal also showed the same optimum pH (i.e., 6.0), while LHyal-$(GGGS)_6$-Sed1p exhibited slightly higher relative activity

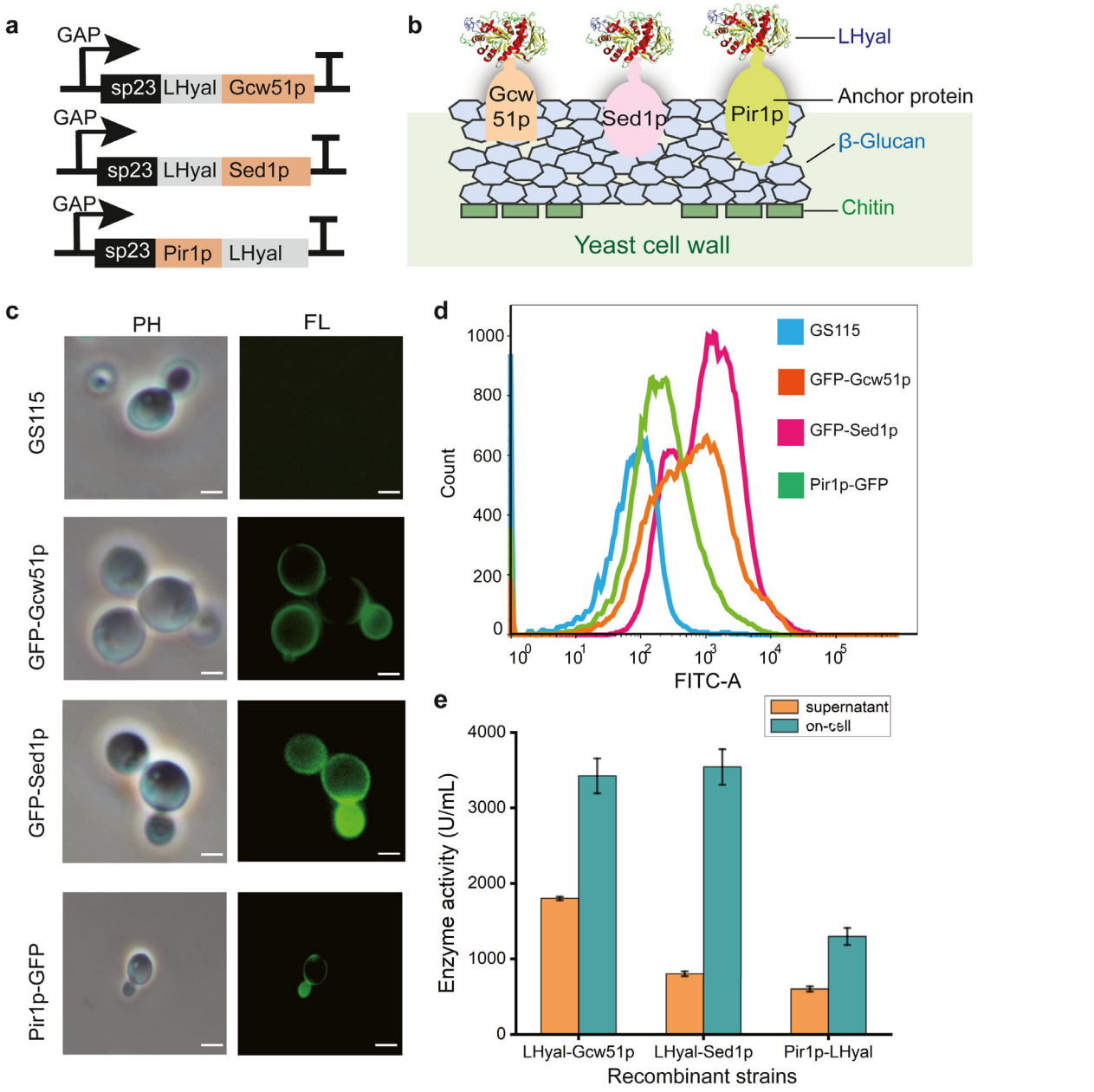

Fig. 1. Selection of anchor proteins for yeast surface display of LHyal. **a.** Construction of LHyal yeast surface display expression cassettes. **b.** Schematic representations of LHyal displayed on the yeast surface using different anchor proteins (cell wall proteins). **c.** Fluorescence microscopic analysis of *P. pastoris* cells expressing GFP-Gcw51p, GFP-Sed1p, and Pir1p-GFP. *P. pastoris* GS115 was used as a control. Scale bars indicate 2.5 μm. **d.** Flow cytometry analysis of *P. pastoris* cells expressing GFP-Gcw51p, GFP-Sed1p, and Pir1p-GFP. *P. pastoris* GS115 was used as a control. **e** Enzyme activity measurements of LHyal released into the culture broth (supernatant) or displayed on the cell surface (on-cell) by Gcw51p, Sed1p, and Pir1p. Data are expressed as mean ± standard deviation of three measurements. Error bars represent SD.

across a range of different pH values (Fig. 4b). Given that many industrial processes may not be performed at optimal pH and temperature, increased tolerance of differences in pH and temperature would make surface-displayed LHyal-$(GGGS)_6$-Sed1p more suitable for industrial HA degradation.

3.5. Evaluation of the reusability of surface-displayed LHyal

Another consideration when developing surface-displayed LHyal was whether the system could be reused (Fig. 5a). This would not only decrease production costs but would also facilitate the separation of the enzyme (insoluble) from HA oligosaccharides (soluble). To evaluate the reusability of LHyal-$(GGGS)_6$-Sed1p we applied 10^4 U mL^{-1} to a solution of 10 g L^{-1} of HMW-HA. After incubation for 15 min, cells expressing LHyal-$(GGGS)_6$-Sed1p were recovered by centrifugation and used for another round of reactions. The resulting supernatant was then used for an enzymatic activity assay and the process was repeated. After five rounds of recycling, the activity of surface-displayed LHyal-$(GGGS)_6$-Sed1p was still about 90% of its original activity (Fig. 5b). Moreover, we applied 10^4 U mL^{-1} LHyal-$(GGGS)_6$-Sed1p to a solution of 2 g L^{-1} of HMW-HA. After five rounds of reacting (1 h for each cycle) and recycling, the average molecular weights of each cycle of HA products were all decreased from the original 2000 kDa to about 1.6 kDa (Fig. 5c). These results suggest that YSD LHyal is highly reusable.

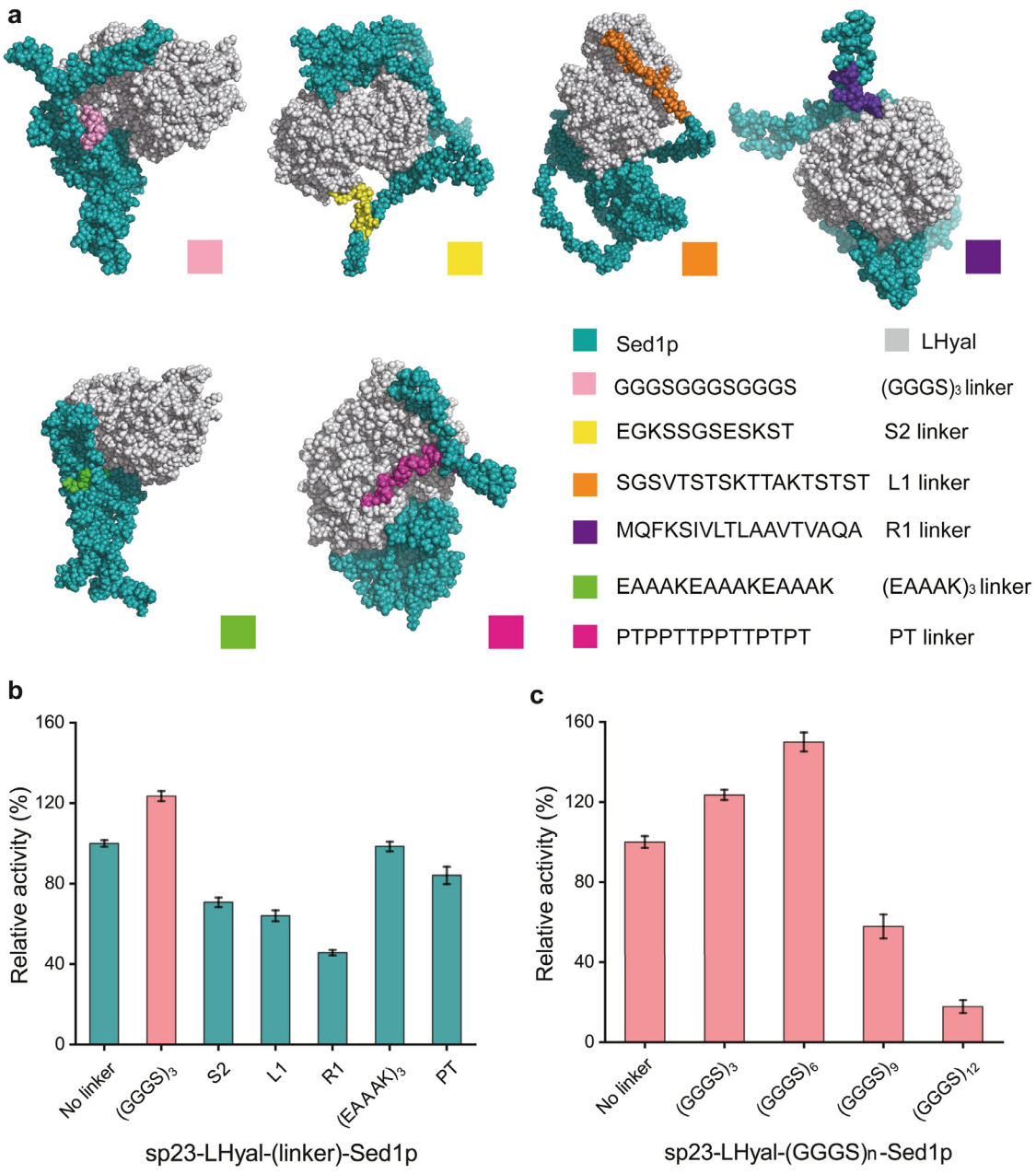

Fig. 2. Screening of protein linkers to enhance the activity of surface-displayed LHyal. **a.** Structural models of LHyal and Sed1p protein hybrids of connected by different linkers. Models were generated using DeepMind AlphaFold [35]. **b.** The impacts of different linker sequences on the surface display efficiency of LHyal-Sed1p. The enzyme activity of LHyal-Sed1p without linker was set as 100%. **c.** Effect of linker length on the activity of yeast surface-displayed LHyal. The enzyme activity of LHyal-Sed1p without linker was set as 100%. Data are expressed as mean ± standard deviation of three measurements. Error bars represent SD.

3.6. Activity of YSD LHyal-$(GGGS)_6$-Sed1p in a fed-batch fermentation test

To test the usefulness of surface-displayed LHyal-$(GGGS)_6$-Sed1p for industrial-scale production of HA oligosaccharides, we performed a high cell density fermentation test using fed-batch fermentation in a 5 L bioreactor. As shown in Fig. 6, the activity of surface-displayed LHyal-$(GGGS)_6$-Sed1p reached 3.58×10^5 U mL^{-1} at 108 h, which was 10-fold higher than the level measured in flask cultures. Such a high level of productivity suggests that surface-displayed LHyal is sufficient for the industrial production of HA oligosaccharides, and that this may simplify the production process and decrease production costs.

4. Discussion

YSD is a very useful tool for protein engineering and has a wide range of biotechnological and biomedical applications. Enzymes displayed on the yeast cell surface combine protein synthesis, secretion, and immobilized in a single step. In this study, cell wall proteins from *S. cerevisiae* and *P. pastoris* were used to display LHyal, which is widely used to hydrolyze HMW-HA to HA oligosaccharides but requires a tedious and cost-intensive purification step.

We found that proteins constructed using the C-terminus of LHyal are more suitable for surface display (Fig. 1e). The enzyme activity of LHyal-Sed1p displayed on cell surface was slightly higher than LHyal-Gcw51p.

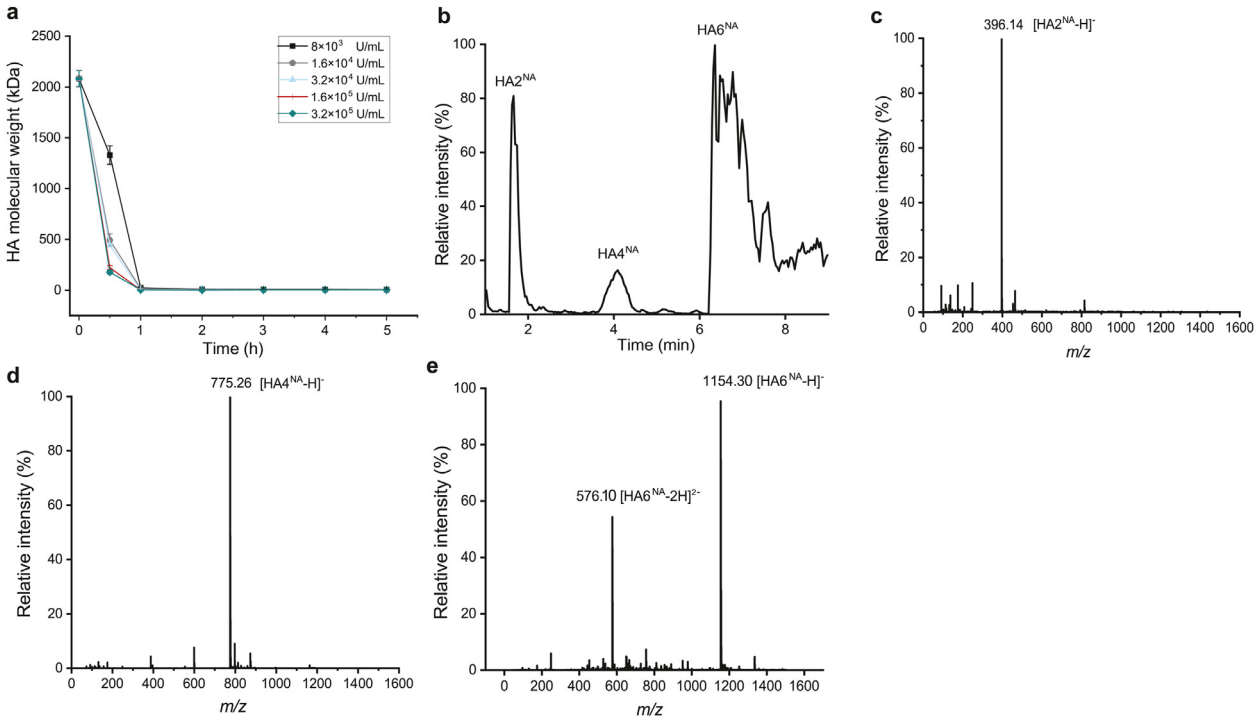

Fig. 3. Hydrolysis of HWM-HA by LHyal-$(GGGS)_6$-Sed1p. **a.** Molecular weight dynamics recorded during HA hydrolysis with the indicated amount of LHyal-$(GGGS)_6$-Sed1p. **b.** Total ion flow chromatogram of the end products of HA hydrolysis catalyzed by LHyal-$(GGGS)_6$-Sed1p; **c.** $HA2^{NA}$ mass spectrum; **d.** $HA4^{NA}$ mass spectrum; **e.** $HA6^{NA}$ mass spectrum.

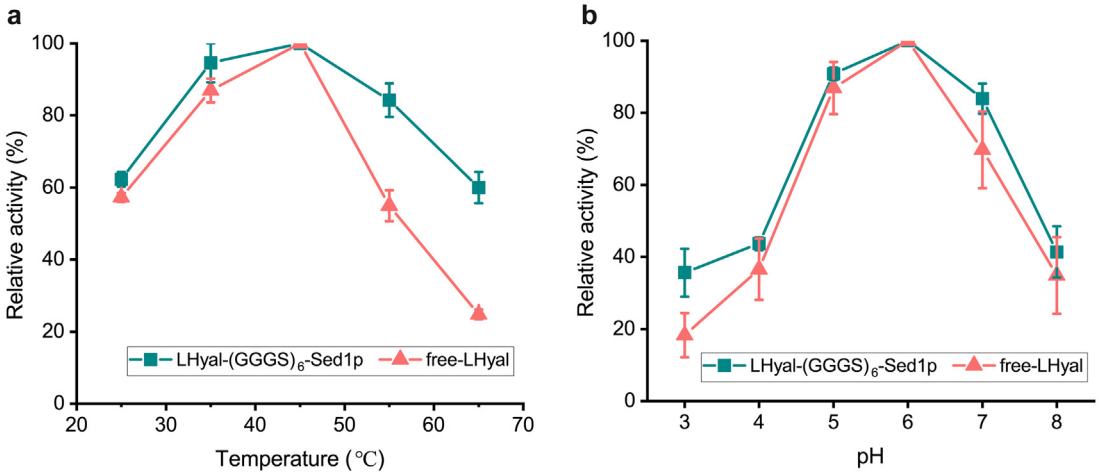

Fig. 4. Enzymatic characterization of yeast surface-displayed LHyal. pH curve **a.** and temperature curve **b.** of LHyal-$(GGGS)_6$-Sed1p. Data are expressed as mean ± standard deviation of three measurements. Error bars represent SD.

However, according to the data of Fig 1e, the ratios of enzymes displayed on cell surface to enzymes released to the supernatant are 4.7 for LHyal-Sed1p and 1.9 for LHyal-Gcw51p, respectively, indicating much better cell wall anchoring capability of Sed1p (Fig. 1e). However, Sed1p is a cell wall protein derived from *S. cerevisiae*, it may slow down the synthesis and secretion of the fused proteins in *P. pastoris*, as the overall activity of LHyal-Gcw51p is higher than LHyal-Sed1p (Fig. 1e). In particular, we found that the conformation of the target enzyme and its interactions with the cell surface anchor protein play an important role in determining enzyme activity [27]. Therefore, we tested several linker peptides to optimize the activity of surface-displayed LHyal (Fig. 2).

Our results showed that surface-displayed LHyal using the flexible linker peptide $(GGGS)_6$ performed the best, showing increased thermal stability at temperatures greater than 45°C. This suggested that surface attachment via $(GGGS)_6$ stabilized the conformation of LHyal. Furthermore, we also found that the activity of surface-displayed LHyal was reduced when the fusion peptide linker was extended to 24 amino acids (Fig. 2c). This effect may be due to detachment of LHyal from the cell wall caused by the weaker mechanical strength of the extended linker.

Finally, after five rounds of reuse, we found that the activity of YSD LHyal on HA hydrolysis decreased slightly (Fig. 5). This means that YSD LHyal not only facilitates enzyme isolation, but also improves the utilization efficiency of LHyal, which should reduce LHyal production costs. We also tested surface-displayed LHyal activity when produced at scale, realizing 3.58×10^5 U mL^{-1} in a 5 L bioreactor. The enzyme activity of free LHyal has been measured in our previous report as 2.12×10^6 UmL^{-1} [11]. which is 5.9 fold of the YSD LHyal. However, the advantage of YSD LHyal is that it does not require protein purification, and

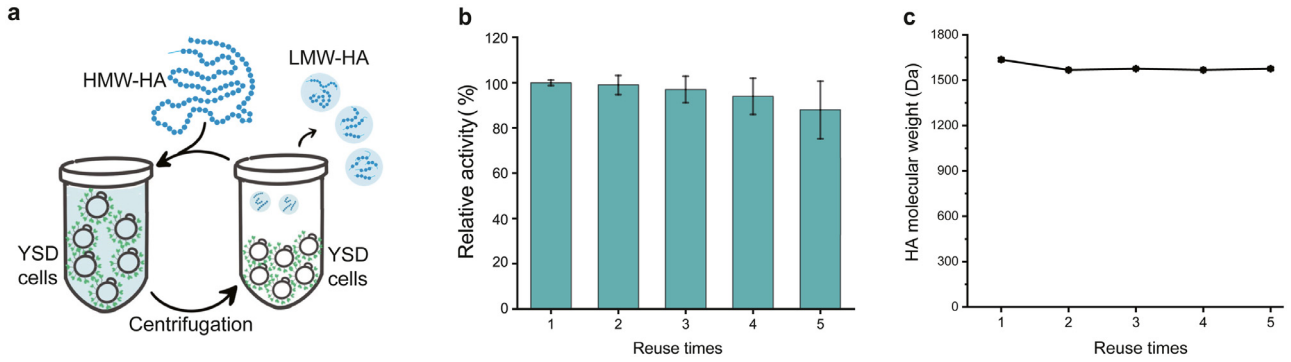

Fig. 5. Reuse of yeast surface-displayed LHyal to depolymerize HA. **a.** Graphical representation to show how to recover and reuse the cells displaying LHyal-$(GGGS)_6$-Sed1p for HA hydrolysis. **b.** Relative enzyme activity measurement for each reuse cycle of LHyal-$(GGGS)_6$-Sed1p. The initial enzyme activity was set as 100%. **c.** The molecular wegiht of HA for each reuse cycle of LHyal-$(GGGS)_6$-Sed1p. Data are expressed as mean ± standard deviation of three measurements. Error bars represent SD.

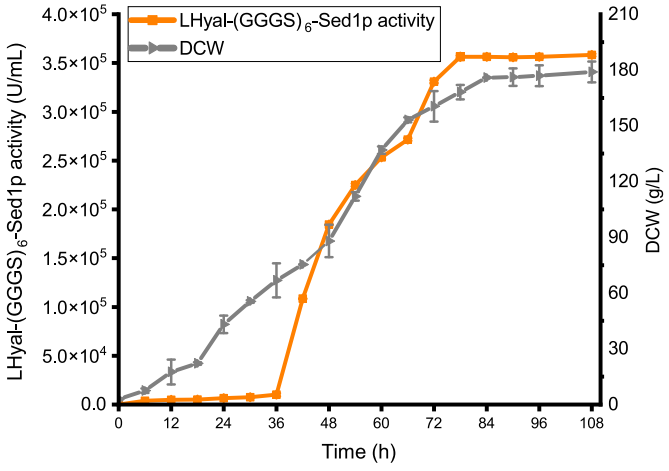

Fig. 6. Production of yeast surface-displayed LHyal using fed-batch fermentation. The recombinant *P. pastoris* strain carrying plasmid pGAP(m)-*LHyal*-$(GGGS)_6$-*Sed1p* was cultivated in a 5 L bioreactor using a fed-batch strategy described in the Materials and Methods section. Time courses of dry cell weight (DCW) and the enzyme activity of surface-displayed LHyal were recorded.

the cells can be reused after a quick centrifugation. The effectiveness of this experiment demonstrates the feasibility of large-scale production of HA oligosaccharides at a low production cost.

Ethical approval

This article does not contain any studies with human participants or animals performed by any of the authors.

Declaration of Competing Interest

The authors declare that they have no known competing financial interests or personal relationships that could have appeared to influence the work reported in this paper.

Acknowledgements

This work was financially supported by the National Natural Science Foundation of China (32000058), the Jiangsu Province Natural Science Fund for Distinguished Young Scholars (BK20200025) and the National Key Research and Development Program of China (2021YFC2103100).

References

[1] J. Necas, et al., Hyaluronic acid (hyaluronan): a review, Veterinární Medicína 53 (8) (2008) 397–411, doi:10.17221/1930-vetmed.
[2] P. Snetkov, et al., Hyaluronic acid: the influence of molecular weight on structural, physical, physico-chemical, and degradable properties of biopolymer, Polymers 12 (8) (2020), doi:10.3390/polym12081800.
[3] M. Hashimoto, K. Maeda, New functions of low-molecular-weight hyaluronic acid on epidermis filaggrin production and degradation, Cosmetics 8 (4) (2021), doi:10.3390/cosmetics8040118.
[4] V. Nobile, et al., Anti-aging and filling efficacy of six types hyaluronic acid based dermo-cosmetic treatment: double blind, randomized clinical trial of efficacy and safety, J. Cosmet. Dermatol. 13 (4) (2014) 277–287, doi:10.1111/jocd.12120.
[5] X. Fu, et al., A general strategy for the synthesis of homogeneous hyaluronan conjugates and their biological applications, Chem. Commun. 53 (25) (2017) 3555–3558, doi:10.1039/c6cc09431g.
[6] B. Pang, et al., Enzymatic production of low-molecular-weight hyaluronan and its oligosaccharides: a review and prospects, J. Agric. Food Chem. 70 (44) (2022) 14129–14139, doi:10.1021/acs.jafc.2c05709.
[7] A. Linker, P. Hoffman, K. Meyer, The hyaluronidase of the leech: an endoglucuronidase, Nature 180 (4590) (1957) 810–811, doi:10.1038/180810b0.
[8] P. Jin, et al., High-yield novel leech hyaluronidase to expedite the preparation of specific hyaluronan oligomers, Sci. Rep. 4 (2014) 4471, doi:10.1038/srep04471.
[9] P. Yuan, et al., Enzymatic production of specifically distributed hyaluronan oligosaccharides, Carbohydr. Polym. 129 (2015) 194–200, doi:10.1016/j.carbpol.2015.04.068.
[10] Z. Kang, N. Zhang, Y. Zhang, Enhanced production of leech hyaluronidase by optimizing secretion and cultivation in Pichia pastoris, Appl. Microbiol. Biotechnol. 100 (2) (2016) 707–717, doi:10.1007/s00253-015-7056-5.
[11] H. Huang, et al., High-level constitutive expression of leech hyaluronidase with combined strategies in recombinant Pichia pastoris, Appl. Microbiol. Biotechnol. 104 (4) (2020) 1621–1632, doi:10.1007/s00253-019-10282-7.
[12] H. Huang, et al., Structure and cleavage pattern of a hyaluronate 3-glycanohydrolase in the glycoside hydrolase 79 family, Carbohydr. Polym. 277 (2022) 118838, doi:10.1016/j.carbpol.2021.118838.
[13] J. He, et al., Construction of saturated odd- and even-numbered hyaluronan oligosaccharide building block library, Carbohydr. Polym. 231 (2020) 115700, doi:10.1016/j.carbpol.2019.115700.
[14] M. Lv, et al., Characterisation of separated end hyaluronan oligosaccharides from leech hyaluronidase and evaluation of angiogenesis, Carbohydr. Polym. 142 (2016) 309–316, doi:10.1016/j.carbpol.2016.01.052.
[15] V.L. Sirisha, A. Jain, A. Jain, Enzyme immobilization: an overview on methods, support material, and applications of immobilized enzymes, Adv. Food. Nutr. Res. 79 (2016) 179–211, doi:10.1016/bs.afnr.2016.07.004.
[16] D.-M. Liu, J. Chen, Y.-P. Shi, Advances on methods and easy separated support materials for enzymes immobilization, TrAC Trends Anal. Chem. 102 (2018) 332–342, doi:10.1016/j.trac.2018.03.011.
[17] A.M. Vieira Gomes, et al., Comparison of yeasts as hosts for recombinant protein production, Microorganisms 6 (2) (2018), doi:10.3390/microorganisms6020038.
[18] G. Li, et al., Construction of a linker library with widely controllable flexibility for fusion protein design, Appl. Microbiol. Biotechnol. 100 (1) (2016) 215–225, doi:10.1007/s00253-015-6985-3.
[19] S. Li, et al., A highly efficient indirect P. pastoris surface display method based on the CL7/Im7 ultra-high-affinity system, Molecules 24 (8) (2019), doi:10.3390/molecules24081483.
[20] M. Ecker, et al., Pir proteins of Saccharomyces cerevisiae are attached to beta-1,3-glucan by a new protein-carbohydrate linkage, J. Biol. Chem. 281 (17) (2006) 11523–11529, doi:10.1074/jbc.M600314200.
[21] R.E. Bird, et al., Single-chain antigen-binding proteins, Science 242 (4877) (1988) 423–426, doi:10.1126/science.3140379.

[22] C. Roth, et al., Structural insight into industrially relevant glucoamylases: flexible positions of starch-binding domains, Acta Crystallogr. D Struct. Biol. 74 (Pt 5) (2018) 463–470, doi:10.1107/S2059798318004989.
[23] K. De Schutter, et al., Genome sequence of the recombinant protein production host Pichia pastoris, Nat. Biotechnol. 27 (6) (2009) 561–566, doi:10.1038/nbt.1544.
[24] M. Kavoosi, et al., Strategy for selecting and characterizing linker peptides for CBM9-tagged fusion proteins expressed in Escherichia coli, Biotechnol. Bioeng. 98 (3) (2007) 599–610, doi:10.1002/bit.21396.
[25] Y. Wang, et al., Eliminating the capsule-like layer to promote glucose uptake for hyaluronan production by engineered Corynebacterium glutamicum, Nat. Commun. 11 (1) (2020) 3120, doi:10.1038/s41467-020-16962-7.
[26] S. Hu, et al., Engineering the probiotic bacterium Escherichia coli Nissle 1917 as an efficient cell factory for heparosan biosynthesis, Enzyme Microb. Technol. 158 (2022) 110038, doi:10.1016/j.enzmictec.2022.110038.
[27] K.V. Teymennet-Ramirez, F. Martinez-Morales, M.R. Trejo-Hernandez, Yeast surface display system: strategies for improvement and biotechnological applications, Front. Bioeng. Biotechnol. 9 (2021) 794742, doi:10.3389/fbioe.2021.794742.
[28] C.J.G. Cruz, et al., Malarial antibody detection with an engineered yeast agglutination assay, ACS Synth. Biol. 11 (9) (2022) 2938–2946, doi:10.1021/acssynbio.2c00160.
[29] Z.Y. Keck, et al., Isolation of HCV neutralizing antibodies by yeast display, Methods Mol. Biol. 1911 (2019) 395–419, doi:10.1007/978-1-4939-8976-8_27.
[30] C. Zhang, et al., Saccharomyces cerevisiae cell surface display technology: strategies for improvement and applications, Front. Bioeng. Biotechnol. 10 (2022) 1056804, doi:10.3389/fbioe.2022.1056804.
[31] M. Lozancic, et al., Systematic comparison of cell wall-related proteins of different yeasts, J. Fungi 7 (2) (2021), doi:10.3390/jof7020128.
[32] I. Hagen, et al., Sed1p and Srl1p are required to compensate for cell wall instability in Saccharomyces cerevisiae mutants defective in multiple GPI-anchored mannoproteins, Mol. Microbiol. 52 (5) (2004) 1413–1425, doi:10.1111/j.1365-2958.2004.04064.x.
[33] X.J. Yu, et al., Surface display of acid protease on the cells of Yarrowia lipolytica for milk clotting, Appl. Microbiol. Biotechnol. 87 (2) (2010) 669–677, doi:10.1007/s00253-010-2549-8.
[34] H. Chen, et al., Effect of linker length and flexibility on the clostridium thermocellum esterase displayed on Bacillus subtilis spores, Appl. Biochem. Biotechnol. 182 (1) (2017) 168–180, doi:10.1007/s12010-016-2318-y.
[35] M. Varadi, et al., AlphaFold protein structure database: massively expanding the structural coverage of protein-sequence space with high-accuracy models, Nucleic Acids Res. 50 (D1) (2022) D439–D444, doi:10.1093/nar/gkab1061.
[36] S. Mingmongkolchai, W. Panbangred, Display of Escherichia coli phytase on the surface of Bacillus subtilis spore using CotG as an anchor protein, Appl. Biochem. Biotechnol. 187 (3) (2019) 838–855, doi:10.1007/s12010-018-2855-7.
[37] J. Ullah, et al., Impact of orientation and flexibility of peptide linkers on T. maritima lipase Tm1350 displayed on Bacillus subtilis spores surface using CotB as fusion partner, World J. Microbiol. Biotechnol. 33 (9) (2017), doi:10.1007/s11274-017-2327-1.
[38] F. Breinig, M.J. Schmitt, Spacer-elongated cell wall fusion proteins improve cell surface expression in the yeast Saccharomyces cerevisiae, Appl. Microbiol. Biotechnol. 58 (5) (2002) 637–644, doi:10.1007/s00253-002-0939-2.